

An Interpretable Deep Learning Approach to Detect Alzheimer Using MRI Images

by

Farhan Anzum Oni
19101048

Kazi Sazzad Hossain Sayem
19301155

Mushfiqur Rahman
19301149

Sanjida Kabir
18301225

Fardeen Yousuf Bhuiyan
18201041

A thesis submitted to the Department of Computer Science and Engineering
in partial fulfillment of the requirements for the degree of
B.Sc. in Computer Science and Engineering

Department of Computer Science and Engineering
School of Data and Sciences
Brac University
January 2023

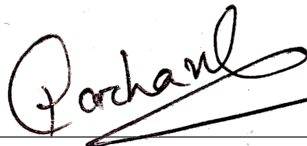
© 2023. Brac University
All rights reserved.

Declaration

It is hereby declared that

1. The thesis submitted is my/our own original work while completing degree at Brac University.
2. The thesis does not contain material previously published or written by a third party, except where this is appropriately cited through full and accurate referencing.
3. The thesis does not contain material that has been accepted or submitted, for any other degree or diploma at a university or other institution.
4. We have acknowledged all main sources of help.

Student's Full Name & Signature:



Farhan Anzum Oni
19101048



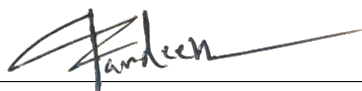
Kazi Sazzad Hossain Sayem
19301155



Mushfiqur Rahman
19301149



Sanjida Kabir
18301225



Fardeen Yousuf Bhuiyan
18201041

Approval

The thesis titled “An Interpretable Deep Learning Approach to Detect Alzheimer Using MRI Images ” submitted by

1. Farhan Anzum Oni (19101048)
2. Kazi Sazzad Hossain Sayem (19301155)
3. Mushfiqur Rahman (19301149)
4. Sanjida Kabir (18301225)
5. Fardeen Yousuf Bhuiyan (18201041)

Of Fall, 2022 has been accepted as satisfactory in partial fulfillment of the requirement for the degree of B.Sc. in Computer Science and Engineering on January 19, 2023.

Examining Committee:

Supervisor:
(Member)

Dr. Md. Ashraful Alam, PhD
Assistant Professor
Department of Computer Science and Engineering
BRAC University

Thesis Coordinator:
(Member)

Dr. Md. Golam Rabiul Alam
Professor
Department of Computer Science and Engineering
Brac University

Head of Department:
(Chair)

Sadia Hamid Kazi
Chairperson and Associate Professor
Department of Computer Science and Engineering
Brac University

Abstract

Alzheimer’s disease (AD) is a serious neurological condition that causes loss of long-term memory, cognitive difficulties, disorientation, inconsistent behavior, and eventually death. Also, AD is caused by the destruction of brain cells that are responsible for proper brain function. The main focus of our research is to provide an efficient model for the rapid diagnosis of Alzheimer’s disease. In this research, we design and demonstrate an interpretable deep-learning approach to detect Alzheimer’s using MRI images. For the experiment, brain MRIs are utilized, and by using this data, the model is able to determine the disease. Additionally, this model is designed based on multiclass classification (MildDemented, ModerateDemented, NonDemented, VeryMildDemented) for helping patients belonging to different phases of Alzheimer’s disease. For this research, we experimented with four different architectures of Convolutional Neural Networks. From the models, we obtained an accuracy of 92.65% for VGG-19, 89.18% for DenseNet-169, 87.84% for ResNet-50 V2, and 80.10% for Inception V3. By comparing and contrasting the performance of the models, the result can be improved by up to 92.65%, and it is decided to implement the best-performing architecture (VGG19) into the system. Although there was a lack of data and it was difficult to tell the difference between a brain suffering from Alzheimer’s disease and a normal brain, the findings obtained revealed accurate identification and categorization of Alzheimer’s disease and its phases. Lastly, GradCam (Gradient-Weighted Class Activation Mapping) is implemented to make the application of Explainable AI(XAI) apparent. Therefore, the proposed system would enable the detection and interpretation of Alzheimer’s disease effectively.

Keywords

MRI, Deep Learning, Convolutional Neural Networks (CNN), Multiclass Classification Approach, VGG-19, ResNet50 V2, DenseNet-169, Inception V3, Augmentation, Explainable AI (XAI), Gradient-Weighted Class Activation Mapping(GradCam).

Acknowledgement

Firstly, all praise to the Great Allah for whom our thesis has been completed without any major interruption.

Secondly, to our supervisor Dr.Md.Ashraful Alam sir for his consistent support and valuable advice in our work. He helped us whenever we needed help.

And finally to our parents without their throughout support it may not be possible. With their kind support and prayer, we are now on the verge of our graduation.

Table of Contents

Declaration	i
Approval	ii
Abstract	iii
Acknowledgment	iv
Table of Contents	v
List of Figures	vii
List of Tables	viii
Nomenclature	viii
1 Introduction	1
1.1 Overview	1
1.2 Problem Statement	3
1.3 Research Objectives	4
2 Literature Review	6
2.1 Related Works	6
3 Methodology	11
3.1 Working Process	11
3.2 Dataset	12
3.2.1 Data Sample	12
3.2.2 Data Classification	13
3.2.3 Training Set	13
3.2.4 Validation Set	13
3.2.5 Testing Set	14
3.3 Data Pre-processing	14
3.3.1 Image Resizing	14
3.3.2 Normalization and Scaling of Images	14
3.3.3 Data Augmentation	14
3.4 Used Architectures	15
3.4.1 Visual Geometry Group (VGG-19)	15
3.4.2 Inception V3	16
3.4.3 Residual Networks (ResNet-50 V2)	17

3.4.4	DenseNet-169	18
3.4.5	Explainable AI (XAI)	19
3.4.6	Grad-CAM	19
4	Implementation	21
4.1	System Configuration	21
4.2	Experimental Setup	21
4.3	Performance Matrices	22
4.3.1	Confusion Matrix	22
4.3.2	Classification Report	22
5	Result Analysis and Experimental Evaluation	24
5.1	Result Analysis	24
5.1.1	Performance Curve(s)	24
5.1.2	Confusion Matrix	26
5.1.3	Performance Evaluation	28
5.2	Comparison between the Deep Learning Models	29
5.2.1	Result Metrics	31
5.3	Result Analysis with Grad-CAM	31
6	Conclusion	33
6.1	Conclusion	33
6.2	Limitations	33
6.3	Future Work	34
	Bibliography	34

List of Figures

3.1	<i>Workflow Diagram</i>	11
3.2	<i>Sample Data from the Dataset</i>	12
3.3	<i>Classification of our Dataset</i>	13
3.4	<i>Augmented Images of Different Classes</i>	15
3.5	<i>An example of the VGG-19 model's custom network design [14]</i>	15
3.6	<i>Module of inception that includes dimension reduction</i>	16
3.7	<i>Inception module with dimension reduction</i>	16
3.8	<i>Residual Learning: a Building block</i>	17
3.9	<i>The Internal Architecture of ResNet-50 V2</i>	18
3.10	<i>The Architecture of DenseNet-169</i>	19
3.11	<i>Grad-CAM Architecture [10]</i>	20
5.1	<i>VGG-19 Model's Metric Visualization</i>	24
5.2	<i>Inception-V3 Model's Metric Visualization</i>	25
5.3	<i>Resnet-50 V2 Model's Metric Visualization</i>	25
5.4	<i>DenseNet-169 Model's Metric Visualization</i>	25
5.5	<i>VGG-19 Confusion Matrix</i>	26
5.6	<i>Inception-V3 Confusion Matrix</i>	27
5.7	<i>ResNet50 V2 Confusion Matrix</i>	27
5.8	<i>DenseNet-169 Confusion Matrix</i>	28
5.9	<i>Accuracy evaluations of four different models</i>	30
5.10	<i>Precision evaluations of four different models</i>	30
5.11	<i>F1 Score evaluations of four different models</i>	30
5.12	<i>Recall evaluations of four different models</i>	31
5.13	<i>Result Metrics for best fit model(VGG-19)</i>	31
5.14	<i>Grad-CAM interpretation of the prediction made by VGG19 when an image of (a) Non-Demented, (b) Mild-Demented, and (c) Very Mild-Demented is provided as input</i>	32

List of Tables

5.1	TABLE 1	29
5.2	TABLE 2	29
5.3	TABLE 3	29
5.4	TABLE 4	29

Chapter 1

Introduction

1.1 Overview

Alzheimer's disease, a common cause of dementia in elderly individuals, destroys one's cognitive ability and weakens it gradually. Also, it is the most prominent neurological condition that damages the brain permanently. Dr. Alois Alzheimer, invented Alzheimer's disease in 1906, by detecting damages in a woman's brain tissues. That woman died from this disease, and the disease was named after its inventor. Dr. Alois invented irregular cell clumps and clotting cell bundles. According to medical science, those are denoted amyloid and neurofibrillary plaques. At the same time, Alzheimer's disease hinders the capacity to concentrate, steadily lessening the patient's memory and hampering their day-to-day life. [27] Alzheimer's disease is an illness that becomes worse over time. Significantly impaired is one of the early and prevalent signs of Alzheimer's disease. This could be a symptom of a stroke, therefore anyone experiencing it should see a doctor immediately. Alzheimer's disease results in psychological or behavioral changes, memory lapses, intellectual disability, identification difficulty, communication with others, thinking difficulties, and other symptoms. Moreover, being older doesn't always mean that the condition gets worse, though Alzheimer's disease is recognized to harm those aged 65 and beyond. Unfortunately, we cannot deny the reality that Alzheimer's disease or different kinds of dementia claim the lives of 1 in 3 old individuals, and in comparison, this belongs to a greater position than the number of breast cancer and prostate cancer altogether. [3]

In this era, this disease is one of the most alarming difficulties in medical science. Because of the intensity of the last phase, it might cause his death in addition to deteriorating his memory. Currently, it is a chronic problem among adults. As there is no absolute treatment for those patients, the only strategy is to extend their lives while dealing with this chronic disease and to diagnose it as immediately and precisely as possible, which might help them to take the necessary steps when they're required. Also, based on the most recent (2020) WHO statistics, the mortality rate of Alzheimer's and other dementia-affected people hit 14,993, or 2.09%, of total deaths in Bangladesh. The adult mortality rate is 13.89 per 100,000 people, which places Bangladesh in 142nd place worldwide, though there isn't a lot of study or data available in this field in our country. [25]

Furthermore, we are aware that emerging nations often have a larger population. Therefore, there is an issue of public wellness since there are a lot of older individuals and a growing number of AD sufferers. Cognitive function gradually deteriorates with AD, which impairs the brain's ability to learn and reason. Depending on the severity of the condition, AD goes through different phases. Also, it can range from mild to severe. Mid-stage indications might create problems with financial transactions, persistently repeating the same question, roaming, and having problems, along with physical and psychological changes. [2]

A patient can function actively while Alzheimer's disease is in its early stages. That individual remains able to drive, operate, and interact with others. Likewise, an individual could suffer from memory impairment, which results in losing track of similar terms or where to find everyday necessities. At this phase of the disease, the signs might not be as those of Alzheimer's disease. However, family members and acquaintances can comprehend their condition, and physicians can identify the indications using the right testing equipment. In the same manner, a mildly affected human might mess up with the common terms. Furthermore, they behave oddly and react weirdly when they get irritated, but the fact is that previously they were not this type. A human with moderate illness reacts strangely and faces hallucinations. After that, badly afflicted individuals rely on others for their daily work, and they are unable to interact with others. Day by day, their condition deteriorates, so they need more and more attention. In this phase, people who are suffering can perform their regular work with others' support. Because of the lack of perfect brain function, their normal body movement is hampered, so those patients spend the majority of their time lying on the bed. So, we can see clearly that a quick and accurate diagnosis is crucial in order to handle this. The signs of dementia get worse when it is in the final stage. Additionally, those patients lose their capacity to respond to the environment and conduct their activities and communication. Day by day, their lives get more difficult to handle. [13]

As memory and intellectual functions deteriorate, behavioral variation takes place, which demands meticulous therapy. At this severe phase, patients are counting their last days, so healthcare practitioners choose many support systems including pain management, to concentrate on the patient's peace. As per Alzheimer Disease International, approximately 44 million individuals in the world suffer from AD or different types of dementia. [12] Moreover, the developed nations in the world consider AD to be a threat to the economy. Also, it is an alarming situation for the general population of our country, as ours is a highly populated nation and the people are not concerned about this disease.

In this research, we describe and consider different methods for estimating and categorizing human MRI scans into the following four categories, which are very mild demented, mild demented, moderately demented, and non-demented. In order to identify Alzheimer's disease using MRI data, fragmentation and categorization of pictures are crucial. Determining the various phases of dementia in its physical entity would aid in treating it at different phases, as we feel it is crucial to recognize the symptoms as soon as feasible. Here, we evaluate ResNet-50 V2, Inception V3, Densenet169, and Explainable AI (XAI), and those perform well on our dataset. Due

to the importance of early Alzheimer’s disease diagnosis to our research, we will be analyzing the images and data in a way that maximizes precision and accuracy. Using appropriate CNN architectures, we produce more appropriate outcomes with higher efficiency for our study on the identification and categorization of AD and its phase than in earlier studies. In our study, we employed an MRI image dataset that behaved admirably and produced better outcomes.

1.2 Problem Statement

Alzheimer’s disease is the leading cause of dementia globally; more than 55% affected by dementia reside in low- and middle-income countries. There are nearly more than 50 million people who have dementia because of Alzheimer’s disease. A lot more people over the age of 65 are now living around the world. It is estimated that this number would reach over 80 million in the year 2030 and 140 million in the year 2050 [1]. In addition, there are over 9 million new cases of dementia each year across the world, which equals one new case occurring every 3.3 seconds over the duration of a year [29].

Dehydration, starvation, or infection can be fatal in patients with advanced stages of Alzheimer’s disease due to the significant loss of brain function. [18] There is a good possibility that a patient with one of these brain disorders will live after proper treatment if they can be detected early. According to the 2011 World Alzheimer Report, early detection and treatment are crucial strategies for decreasing the treatment gap.[21] Even in the early stages, it is difficult for a doctor to detect the disease and its severity. Therefore, it is imperative to establish a rapid method for determining the kind and severity of an illness. [12]

Alzheimer’s disease requires extensive, costly treatment and supervision. Since people who suffer from Alzheimer’s disease are mentally, and physically exhausted and spend their days in fear of death. To reduce their suffering, working in this field is necessary for this century. Day by day, people do research in this area using machine learning (ML), in which the model experiments with prior data for the purpose of identifying specific diseases. Also, in this situation, proficiency and precision are crucial, but they are very hard to get. Appropriate training for the system is vital since the goal of our study is to diagnose Alzheimer’s disease from a brain MRI. After conducting the study, previous experts in this domain achieved previously unheard-of achievements, but they encountered challenges in putting their findings into practice. It is very time-consuming and hard to perform properly to train the algorithm using AD-impacted brain images to produce a proper assumption. Moreover, applying a method that gives the desired and effective result is essential. Deep learning, a significant approach to machine learning, is required for this study. Even though there is well-developed technology, undesirable situations happen, and many false positive patients get treatment on a regular basis. Actually, the advancement

of a system with greater precision is essential since a test result can have a significant impact on life and decide a patient's fate. Eventually, it might be difficult to add additional features and additional performance since experts are unsure of their viability. Using brain scans and brain disorders as input, we have developed a deep learning methodology that's more effective than anything else on the market right now. This approach also has a higher level of accuracy than earlier ones. We developed a multiclass classifier to diagnose brain diseases, employing deep neural network architectures such as VGG 19, Resnet50 V2, DenseNet 169, and Inception V3. Using an explainable AI (XAI) technique for assessing the disease discovered on the brain image data, it is possible to identify the condition accurately. Lastly, this procedure necessitates a significant amount of additional testing time. Although there are many obstacles, the goal of this study is to solve them by finding solutions, learning about new concepts, and dispelling ambiguity [16].

1.3 Research Objectives

Alzheimer's disease (AD) is well-known because of the significant health concerns it brings and the absence of a sustainable cure. One of the leading causes of mortality in the contemporary period, Alzheimer's disease strikes elderly individuals and exposes them to more viruses like COVID-19. It affects both Bangladesh's population's health status and its economy. In this paper, we develop an effective strategy utilizing deep learning methods for identifying early signs of brain disease. A deep learning model is being developed here that can predict the outcome of brain disease detection using brain images. Although this disease causes irreparable loss, early identification and medication can lower both the fatality rate and the proportion of the loss. Also, a model needs to be more precise, as only quick discovery of the disease does not work effectively without higher accuracy. The following are the objectives of our research.

- Our primary goal is to determine the level of Alzheimer's disease in humans in order to design an excellent predictive model for predicting the severity of the disease.
- Our aim is to create a model which is more effective than existing models and provides better outcomes.
- We are attempting to detect Alzheimer's disease in its early stages using this method so that individuals can benefit from treating it early on and avoid the severe damage it can bring.
- Moreover, the methods that we use can identify and anticipate the potential risks of Alzheimer's disease, and they will supply the essential providers with a larger possibility, which makes them extremely important for the early diagnosis and treatment of the condition.

- With the assistance of this study and appropriate explanation, we hope to substantially enhance the mental and physical well-being of Alzheimer's disease individuals and their families.
- To raise public knowledge of Alzheimer's disease, this study intends to. When a patient visits for a prognosis of disease or treatment, it will be helpful to work with them and understand the estimation of the critical levels of the expansion of dementia inside that person. This way, patients can take the inevitable precautions to avoid the final stage of Alzheimer's Disease in the future.

Chapter 2

Literature Review

2.1 Related Works

Yousif A. Hamda, Konstantin Simonov, and Mohammad B. Naeem proposed a technique for detecting the edges of a patient's brain tumor on an MRI scan[15] . For an appropriate diagnosis using BCET, this approach contains some noise removal capabilities followed by enhancement features. Next, clustering using the Fuzzy c-Means (FCM) approach is applied to the second stage's output. In the final step, the Canny edge detection method identifies the more delicate edges. For the experimental study, we employed photos of Alzheimer's disease with varying locations, pathologies, shapes, sizes, and densities, as well as the size of the damaged tissue surrounding the tumor space. Finally, software such as MATLAB is used to find and remove malignancies from brain MRI scans. Studies of the empirical material using the proposed methodology have shown some resistance to noise in the results obtained. It was also discovered that the accuracy of solving geometric analysis and segmentation difficulties was up to 10-15 percent better than the comparable expert estimations in specific situations of pathological tumors.

Martin Cenek, Masa Hu, Gerald York, and Spencer Dahl stated that it is presented in this research how to use image processing techniques to diagnose brain pathology [32]. Images are processed to gain insight into the workings of the brain. This method displays the information stored in the brain during processing. The soft tissues of the brain can be examined via radiography, MRI, nuclear medicine, ultrasound, and infrared imaging. Training algorithms for spotting abnormalities in the brain are commonly done using magnetic resonance imaging (MRI). An axial anatomical plane slice is a horizontal cross-section of the brain separated from the next by 0.2 to 6.0 mm along the vertical axis by an MRI of the brain (spinal axis). The number of images in the final picture sets can range from 170 to 1,500, depending on the number of imaging devices used and the desired amount of brain imaging.

In this research paper, neuroimaging biomarkers are being utilized as a noninvasive way of identifying Alzheimer's disease and dementia. This paper is a smaller component of a more extensive body of work. sMRI images were used in some capacity as input for the algorithm that detects Alzheimer's disease. They did this by lowering the magnetic resonance brain imaging with T1 weighted volumetric to a

two-dimensional space using a variety of preprocessing approaches, which they used for three different projections. This allowed them to see the brain in three different ways. The researchers wanted to collect a greater number of MRI samples, thus they merged the OASIS and MIRIAD data sets. They were successful in achieving an accuracy of detection that was 82%, which was the greatest achievable. In order for the proposed model to function appropriately, the MRI scan of the patient's brain does not need to have any additional procedures for the extraction of features or selection of features applied to it. After creating the most effective CNN model that can be made and determining the parameters of the model, the model can then be utilized to analyze new health information without the need for any involvement from a human being [28].

P Gokila Brindha, M Kavinraj, P Manivasakam, and P Prasanth stated that one possible precursor to cancer is abnormal cell expansion in the brain, known as a tumor. MRI scans are the most commonly used method of detecting a brain tumor. MRI images can reveal unusual tissue growth in the brain. Numerous studies have been conducted to diagnose brain tumors using machine learning and deep learning algorithms. When these algorithms are applied to MRI data, they can predict brain tumors in less time and with greater accuracy. The radiologist can benefit from these predictions, which help them make quick decisions. In the proposed work, the performance of a self-defined Artificial Neural Network (ANN) and a Convolution Neural Network (CNN) in detecting the presence of a brain tumor is investigated.[31]

In the paper by Vipin Y. Borole, Sunil S. Nimbhore, and Dr. Seema S. Kawthekar et al., "Image Processing Techniques for Brain Tumor Detection," the researchers have tested their various working principles, and advantages and disadvantages enable them to compete against one another. A modified hybrid median filter or morphology-based denoising can also improve the efficiency of their operations. Hybrid filters, which combine the median and Wiener filters into a single filtering process, are another option. In addition, they have shown expertise in their field.[26]

Roberto Fontana and Mario Agostini describe that, as Alzheimer's disease progresses, mild cognitive impairment (MCI) is accompanied by changes in the activity of brain networks. The search for early biomarkers of network breakdown is just beginning, both in people and in AD mouse models. PS2APP rats with the APP Swedish mutation and the PS2 N141I mutation were studied for the activity of local field potentials in their dentate gyruses. We discovered network hypersynchronicity as early as three months when the amyloid-beta accumulated intracellularly. Beta/Gamma frequency band network hyperactivity was identified in infants at six months of age and amplitude-phase cross-frequency coupling, which is compatible with the disease's histology features. Even though mice expressing either the PS2-N141I or the APP Swedish mutant alone showed signs of hyperactivity and hyper synchronicity, the PS2APP animals aged six months or less showed an increase in cross-frequency coupling immediately before the onset of cognitive impairment. [33]

Research conducted by scientists from the United Kingdom and China used a deep convolutional neural network to try to identify the most helpful features of sMRIs

(DCNN). The information is then put through a severe pipeline of data preprocessing for ease of use. Each output is resliced before it is sent to the DCNN. There are four phases of Alzheimer’s disease that may be recognized, with an average accuracy of 94.% for LMCI vs EMCI, 94.5% for NC vs LMCI, 97.81% for EMCI versus AD, 97.2% for LMCI and AD, and 96.9% for NC versus AD [24]. The research also acknowledges the field’s drawbacks, including how the availability of standard datasets affects CNN’s training accuracy. For this reason, it must be followed by a supervised machine learning technique, such as a support vector machine (SVM). To address this issue, the research proposes a two-stage unsupervised deep learning approach. The first section uses an unsupervised machine learning technique, with the results being classified using an unsupervised classification technique. An unsupervised convolutional neural network (CNN) named PCANet is used to process a feed of 3 orthogonal MRI views, and then the results are classified using a k-means clustering algorithm-based unsupervised classification technique that yields an average accuracy of 92.5% [22].

However, a recent paper that was published in October 2020 illustrates the use of imaging technologies, looking to capitalize on the fact that MRIs reveal significant intellectual volume changes as the brain structure devolves throughout the progress of the disease, and giving 92% of precise figures without a patient’s past records by generating biomarkers for effective diagnosis [23]. This paper was written in response to the fact that MRIs unveil spectacular intellectual volume changes as the brain structure evolves throughout the progression of the disease. Other deep learning algorithms utilizing CNNs or RNNs that do not pre-process neuroimaging data for feature selection have achieved accuracy rates as high as almost more than 95% for AD classification and 85% for MCI conversion prediction [17]. These rates of accuracy were achieved for the classification of AD.

Using MRI data provided by the BraTS, a platform for exploring machine learning methods for brain tumor identification was built by Györfi, Á., Kovács, L., & Szilágyi, L. Moreover, when working with the same preprocessed data, they also compared several ensemble training procedures in a similar situation. A Random Forest (RF) classifier was also utilized, as was an ensemble of simple Adaboost classifiers, an ensemble of artificial neural networks (ANN), and an ensemble of binary decision tree (BDT) algorithms for improved detection. We thoroughly analyzed all 54 low-grade BraTS 2016 tumor sizes. One of every 40 pixels is incorrectly categorized, meaning that 97.5 percent of all algorithms are consistent with each other. Accuracy indicators indicate that all four algorithms evaluated can be used in the decision-making process. They concluded that random forests are the best solution among the known group learning methods because of the minimal fluctuations in accuracy and the runtime criteria [6].

In the research paper by Rohit Bakshi and Alan J. Thompson, an increasing number of cutting-edge MS research and treatment methods are being developed using MRI. In order to determine if advanced MRI techniques can aid in early diagnosis or better phenotyping, they must be tested. Post-processing enhancements should make it easier to extract more valuable data from images. It is expected that magnetic resonance spectroscopy will become more sensitive and specific with increasing field

strengths. This will allow researchers to identify more metabolites. Because of advancements in diffusion imaging, it is becoming easier to determine the functional significance of lesions in specific regions. New magnetic resonance contrast agents may allow for cell-specific imaging. Imaging myelin water fractions can achieve a precise assessment of myelin composition. The sensitivity of ultra-high-field MRI has increased, but new technological challenges have also been introduced. Recent MRI achievements for MS are discussed in this article, along with future developments in imaging the spinal cord, the optic nerve, perfusion MRI, and functional MRI. New MRI technology may make it easier to detect, monitor, and understand the underlying causes of multiple sclerosis (MS) [8].

ADNI researchers performed multisite longitudinal observational studies on healthy older adults, those with mild cognitive impairment (MCI), and people with dementia, as detailed in a report authored by Clifford R. Jack Jr., MD, and Paul Thompson, Ph.D. Clinical and psychometric assessments, as well as biomarkers from MRI, fluorodeoxyglucose positron emission tomography, urine, and CSF, are collected at multiple time points throughout the trial. With time, the data will be unified and shared with researchers everywhere. The purpose of this research is to analyze the ADNI MRI methods currently in use. The ADNI MRI core developed the required standards for the protocol. It took a lot of work to run morphometric analysis on 3D T1-weighted sequences. Small-scale clinical trials were conducted to determine the optimal sequence from among several possibilities built for the platforms of the major manufacturers. ADNI MRI methods are developed to increase scientific value while decreasing participant burden. Researchers believe that the ADNI protocol for standardized MRI across sites and platforms, post-acquisition modifications, and phantom-based monitoring of all scanners can serve as a model for future multi-site studies [4].

According to Robert W. McCarley, Cynthia G. Wible, and Martha E. Shenton's research on structural MRI investigations, schizophrenia is a brain disorder marked by structural alterations and therefore involves more than just a disruption in neurotransmission. From 1987 to May 1998, peer-reviewed papers with a matched control group were investigated. Studies demonstrate that the lateral and third ventricles are enlarged in 77% and 67% of the cases, respectively, whereas the overall brain/intracranial contents are standard in 81% of the cases. Structural Magnetic Resonance studies found abnormalities less frequently, despite evidence of frontal lobe dysfunction, with a reported 55% decrease in volume. In this case, MRI may be unable to detect even small changes in the volume of the frontal lobe. Only around half of the experiments on the parietal and occipital lobes were successful. Most cortical gray matter studies (86 percent) found that volume losses were not uniform but rather more pronounced in specific areas. Studies on the thalamus, corpus callosum, and basal ganglia's subcortical structures, as well as the cavum septum pellucid (which is responsible for swelling in the brain), generate good results in approximately two-thirds of the instances (CSP). On the other hand, an ever-growing body of evidence indicates progressive and neurodegenerative traits that are suggestive of a 2-hit concept of schizophrenia, for which a cellular hypothesis is currently being studied. The overwhelming majority of the evidence pointed in this direction. For instance, the link between clinical symptoms and MRI data is

investigated, as is the mounting evidence that structural abnormalities in affective disorders and schizophrenia disorders are distinct from one another [5].

Chapter 3

Methodology

3.1 Working Process

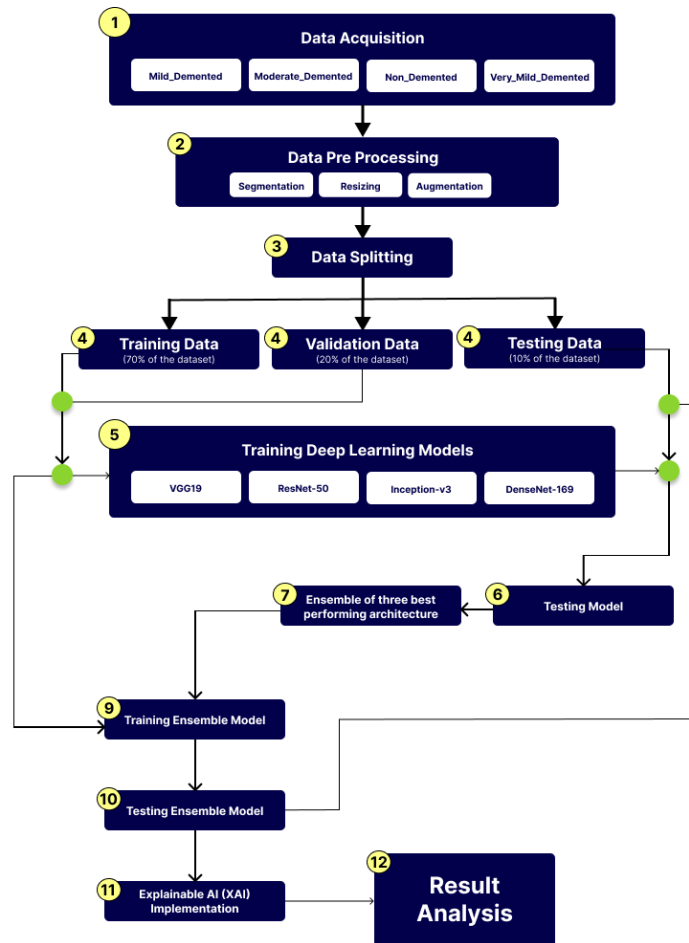


Figure 3.1: *Workflow Diagram*

In the following, Figure 3.1 shows an overview of each step we will take to train and test our model. We will collect and integrate our data to begin. Following that, we perform data preprocessing. After preprocessing, our dataset will be divided

into a 7:2:1 ratio. 70% of our dataset will be used to train the aforementioned deep learning models, while 20% will be used for validation and 10% for testing our existing models. We will conduct our study using various deep-learning models, including VGG19, ResNet-50 V2, Inception-v3, and DenseNet-169. We will then compare the validation accuracy of the models we utilized. Next, we will identify the top three performing designs and combine them for a more efficient result. After that, we will apply Explainable AI (XAI) to the fusion model. Finally, we analyze the data and design a system for detecting brain diseases.

3.2 Dataset

In order to identify early signs of Alzheimer’s disease, we wish to gather datasets of MRI pictures and divide them into four categories. The datasets were first gathered from unreliable websites. To properly identify the early stages of Alzheimer’s disease, however, sophisticated datasets are needed and it is difficult to locate better datasets, such as MRI scans. A variety of datasets, including OASIS and ADNI, are available online. As a result, we looked through these sites to find trustworthy datasets of MRI pictures. If we wish to recognize Alzheimer’s disease, the dataset of MRI pictures must be exceedingly reliable and verified by medical associations. We looked over those datasets and discovered the "Dataset Alzheimer" standard dataset, which is ideal for our research because it has four different image classifications [35]. As a result, we made the decision to employ this dataset in our research.

3.2.1 Data Sample

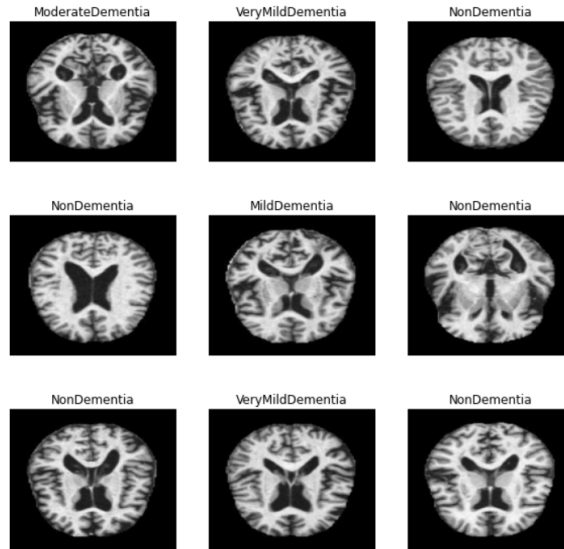


Figure 3.2: *Sample Data from the Dataset*

In the above figure 3.2, there are 4 classes of Alzheimer’s MRI images. Those are the categories according to dementia. Four Classes are MildDementia, ModerateDementia, NonDementia, and VeryMildDementia. There are 3200 affected images and 3200 non-affected images in our normal brain MRI image dataset. In our dataset,

there are 3200 affected images and 3200 non-affected images. For those 3200 affected images, there are Four classes. In the mildly demented class, there are 896 images. In the moderate demented there are 64 images and lastly, in the very mild demented class, there are 2240 images.

3.2.2 Data Classification

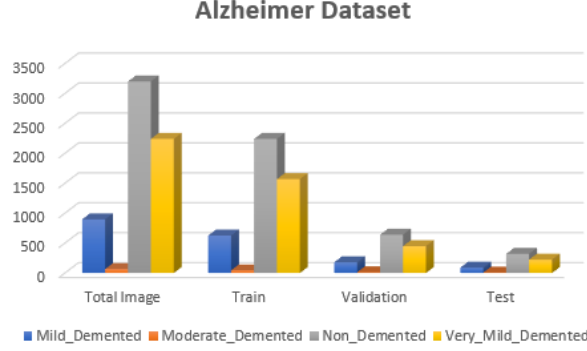


Figure 3.3: *Classification of our Dataset*

3.2.3 Training Set

A dataset used to train a machine-learning model is called a training set. It is used to adjust the model’s parameters—namely, its weights and biases—to the data. When given a set of input-output pairings, the model changes its parameters to reduce the difference between the expected and actual results. Finding a collection of parameters that can generalize effectively to novel, untested data is the aim of training a machine learning model. In other words, the model should be able to predict outcomes accurately for new data. To do this, a representative sample of the data is utilized to train the model, and its performance is then assessed on a separate test set. When training a machine learning model, the training set is of utmost importance. As a result, we choose 70% of the entire dataset as our training set. As a consequence, our dataset contains 4,478 photos across four classifications.

3.2.4 Validation Set

A dataset used to test a machine-learning model while it is being trained is known as a validation set. It is used to fine-tune the model’s hyperparameters, including the regularization coefficient and learning rate. During training, the model’s effectiveness is evaluated using the validation set after each epoch (i.e., pass through the complete dataset). To decide whether to halt training, lower the learning rate, or alter another hyperparameter, the model’s performance on the validation set is employed. The training set, which is used to fit the model’s parameters to the data, is distinct from the validation set. Additionally, it differs from the test set, which is used to assess the model’s ultimate performance following training. It is crucial to utilize a validation set since it enables the model to be adjusted and prevents overfitting to the training set of data. We use 20% of the data as a validation set

after taking the training set. As a consequence, our dataset contains 1,281 photos from four classifications.

3.2.5 Testing Set

A testing set is a dataset used to evaluate a machine-learning model after the training process. It is used to assess the model's performance on new, unseen data. As the judgment becomes more biased when the validity dataset's competency is taken into account in the given model. The training set, which is used to match the model's parameters to the data, is distinct from the test set. Additionally, it differs from the validation set, which is utilized during training to fine-tune the model's hyperparameters. To measure the model's performance on unobserved data, a test set is used. This is crucial since the end result of a machine learning model is to provide precise predictions based on fresh, untested data. By evaluating the model on a test set, it is possible to get a sense of how well the model will perform in the real world. From our selected dataset, we take 10% of the data as a testing set. As a result, we take 641 images of Four Classes of our dataset.

3.3 Data Pre-processing

3.3.1 Image Resizing

To begin with the dataset preprocessing, we wanted to make sure that each image had its own individual id. Next, we've modified the dimensions of every picture to the standard (224 x 224). The photos are then rescaled to 1/255 their original size [9] as part of the dataset's formatting. And we process every single image in the training, validation, and test datasets.

3.3.2 Normalization and Scaling of Images

In order to reduce data duplication, unnecessary picture details are removed from the normalization process. In addition, component analysis was used to ensure consistency throughout this process of data collection. By using principal component analysis (PCA), a large dataset may be reduced in size without losing any of its essential information. It is possible to normalize MRI scans of the brain by generating and combining corresponding flat fields. The use of dynamic flat fields can also reduce normalization errors in projection intensities [1]. In order to do this operation, the ImageDataGenerator application was utilized. Data normalization also occurs when each pixel in a picture is multiplied by the same ratio and then applied to each of the other pixels. In addition, we gathered all of our information from.jpg files including magnetic resonance imaging scans of healthy and diseased human brains.

3.3.3 Data Augmentation

When doing our research on the datasets, we make use of enhancement methods like zooming the images, and flipping and rotating the images. First of all, a horizontal rotation and a right-angle flip were applied to each and every dataset. After that,

the limitations of the zoom method have been increased to almost 0.2. We have used this technique for each and every set of data. This is how we have augmented our data.

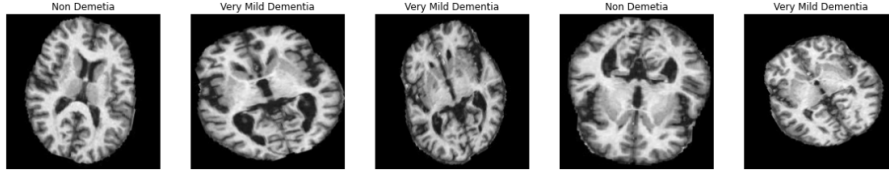


Figure 3.4: *Augmented Images of Different Classes*

3.4 Used Architectures

In our research, we used five architectures, which are VGG-19, ResNet-50 V2, DenseNet-169, Inception V3, and Explainable AI (XAI). The details of this architecture are given below:

3.4.1 Visual Geometry Group (VGG-19)

The VGG-19 network is an intense convolutional neural network. This obtained 92.7 percent top-five test accuracy when using ImageNet, a dataset consisting of over 14 million pictures and 1000 classes, for large-scale image identification. The VGG-19 is a deep-learning model with 19 neural network layers. ImageNet contains a pre-trained network that has been exposed to over a million images. Each filter used a maximum of three by three cells, with a stride of one and a pad of twenty-two [30]. All of the filters in a convolutional neural network are put to good use, with an error rate of only 7.3 percent.

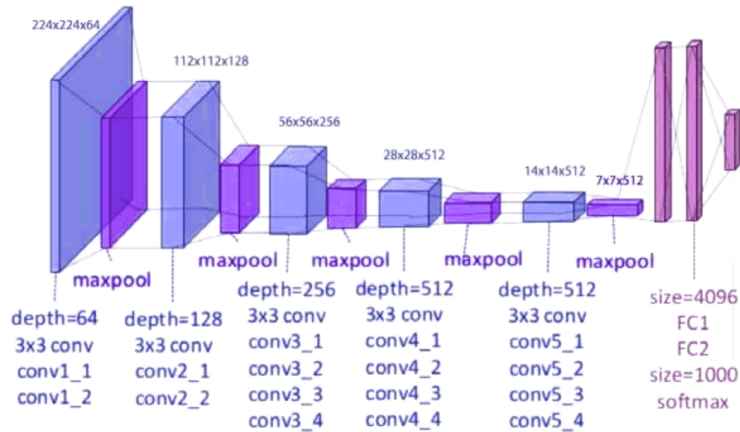


Figure 3.5: *An example of the VGG-19 model's custom network design [14]*

VGG-19, on the other hand, is second in recognition and first in localization because of its 138M features. To help construct this model, we leveraged components of ImageNet. Some of the 19 easy-to-train layers in the VGG-19 include convolutional and fully connected layers, as well as max pooling, dropouts, and fully connected layers. The current version of the VGG-19 model is depicted in Figure 3.5

3.4.2 Inception V3

Instead of going deeper and adding additional convolutional layers on top of each other, the third version of the Inception v3 family uses transfer learning [34] to acquire better classifications. In Inception, many alternative levels were used. The emphasis is on expanding the network rather than improving its base. The expanded model has the capability to change between a wide number of symmetric and asymmetric construction elements, including dropouts, max pool layer, convolutional layers, entirely connected layers, average pooling, and contacts. Both the architecture and the application features use batch normalization. Below is an example of a normal inception module.

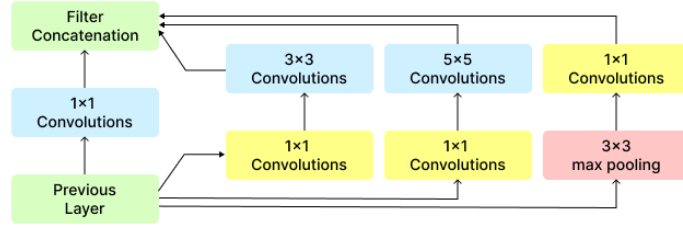


Figure 3.6: *Module of inception that includes dimension reduction*

The Inception Model relies heavily on this fundamental element. Stacking always adds more layers, making the model deeper, and thus subject to the vanishing gradient problem that affects all deep neural networks. Additional filtering was used to make sure no data was lost on the way. Several levels of changes to the module's filter banks reduced complexity, reduced the need for dimension reduction, and reduced the impact of bottlenecks in the representational process. When compared to earlier iterations of Inception, the Regularization Optimizer, Batch Normalization in the Auxiliary Classifiers, 7x7 Convolution layers, and Label Smoothing are just a few of the additional features that we added to Inception v3. To avoid extreme over fitting, the final was inserted. The layered architecture of Inception v3 is shown in a condensed form below, followed by a description of the design in more [34].

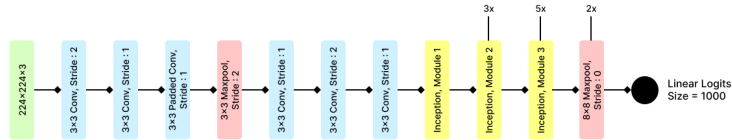


Figure 3.7: *Inception module with dimension reduction*

3.4.3 Residual Networks (ResNet-50 V2)

In 2015, a network called ResNet (residual network) was released and quickly became so successful that it won the ILSVRC visual recognition competition. Over fitting has been reduced by increasing the number of layers in Neural Networks, hence, this approach is becoming more popular. However, the vanishing gradient problem arises at even deeper levels. As the gradient is multiplied as it is back-propagated via the previous levels, it is possible that it will grow smaller. This issue becomes more severe as one progresses further into the layers. Consequently, performance decreases at all layers [36]. Using techniques like "identifying bypass connections," "Jump Connections," and "residual connections," ResNet is able to find and eliminate these issues. Figure 3.6, under "Residual Learning," demonstrates how this strategy is able to bypass the need for some network connections, leading to layer blocks.

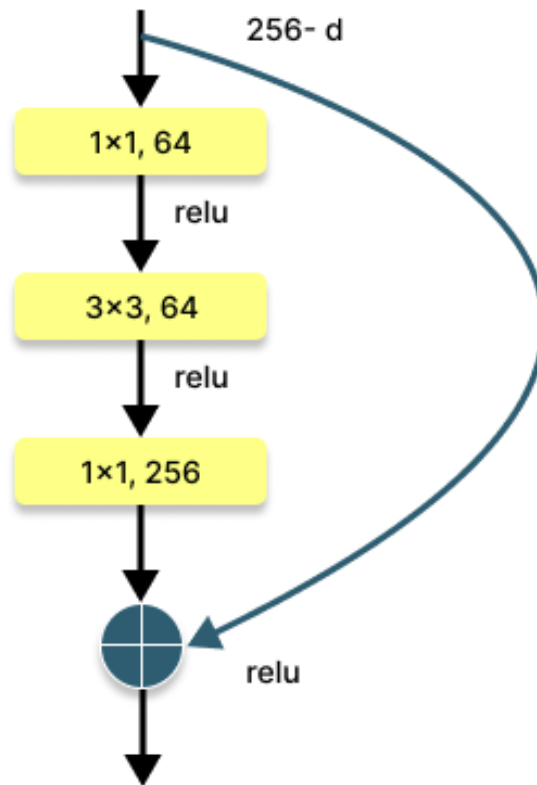


Figure 3.8: *Residual Learning: a Building block*

ResNet 50 V2 is composed of 50 layers: 48 Convolutional layers, 1 max pool layer, and 1 Average pool layer. Each of the four parts of this model—a conversion block and an identification block—makes up the whole. Each of the blocks' 3 convolution layers (as seen in the figure above) uses a 7×7 Kernel for the first convolution and a 3×3 Kernel for the max-pooling[20].

At the first stage of the model, where three residual blocks and three layers are used, batch normalization is commonly deployed. When doing convolution, stride 2 is used to lessen the input and increase the channel size by 1. After each layering step, the

three layers are placed in a block using successive 1x1, 3x3, and 1x1 convolutions. It is the 3x3 layer that functions as a bottleneck, reducing the output dimensions, while the 1x1 levels reduce and immediately restore the data dimensions. The following is a simplified diagram of the construction of the ResNet blocks:

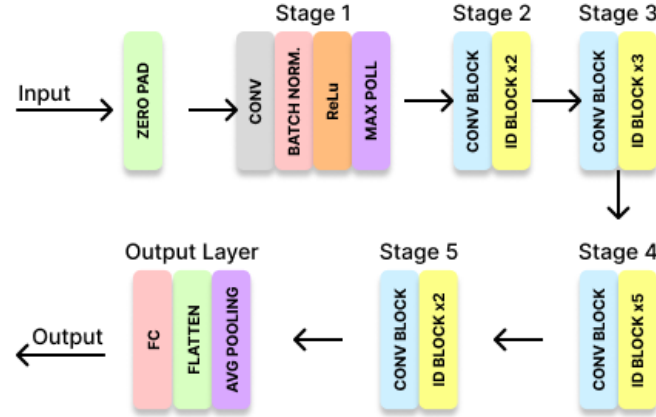


Figure 3.9: *The Internal Architecture of ResNet-50 V2*

3.4.4 DenseNet-169

When it comes to identifying objects in pictures, DenseNet is an innovative new neural network. Model number 169 from the DenseNet Group. The DenseNet team is responsible for the classification of images. The new DenseNet 169 is significantly larger than its predecessors. Instead of utilizing ImageNet, the standard image database for training in DenseNet, we trained, stored, and tested our model using our own image dataset. At this stage, the output from the current layer is appended to the output of the next layer, which will be DenseNet. DenseNet was developed to mitigate the negative effects of the declining gradient on the accuracy of a deep neural network. Due to the distance between the input and output layers, data is corrupted along the way. The network architecture known as DenseNet is considered classical. The newest information suggests that convolutional layers may be more productive and accurate. Possibly very deep if connections between layers are shorter close to inputs and outputs. In this instance, we used DenseNet to feed-forward link each layer to itself. Traditional convolutional networks often make use of L layers. Additionally, the L levels are connected through an L connection. That is, each layer only has one connection to the next higher layer. The network in question contains $L(L+1)/2$ vertices [7]. Each successive layer incorporates data from the prior levels as inputs. This structure's feature maps serve as raw material for all subsequent levels. There are several advantages to using DenseNet. When used, they are effective in resolving the issue of disappearing gradients. It helps with parameter reduction, promotes feature reuse, and increases feature propagation.

Layers	Output Size	DenseNet 169
Convolution	112×112	7×7 conv, Stride 2
Pooling	56×56	3×3 max pool, Stride 2
Dense Block (1)	56×56	$\begin{bmatrix} 1\times 1 \text{ conv} \\ 3\times 3 \text{ conv} \end{bmatrix} \times 6$
Transition Layer (1)	56×56	1×1 conv
	28×28	2×2 Average Pool, Stride 2
Dense Block (2)	28×28	$\begin{bmatrix} 1\times 1 \text{ conv} \\ 3\times 3 \text{ conv} \end{bmatrix} \times 12$
Transition Layer (2)	28×28	1×1 conv
	14×14	2×2 Average Pool, Stride 2
Dense Block (3)	14×14	$\begin{bmatrix} 1\times 1 \text{ conv} \\ 3\times 3 \text{ conv} \end{bmatrix} \times 32$
Transition Layer (3)	14×14	1×1 conv
	7×7	2×2 Average Pool, Stride 2
Dense Block (4)	7×7	$\begin{bmatrix} 1\times 1 \text{ conv} \\ 3\times 3 \text{ conv} \end{bmatrix} \times 32$
Classification Layer	1×1	7×7 global average pool
	1000	1000D fully-connected, softmax

Figure 3.10: *The Architecture of DenseNet-169*

3.4.5 Explainable AI (XAI)

It is difficult to understand how a Neural Network or Machine Learning model comes at its results. The term "black box" is used to describe these types of models because of this. No one knows what's going on within those models or how they're achieving their goals. This means that XAI, or Explainable AI, is required in order to provide an explanation for the actions of deep Neural Network models. It's a device that helps humans understand how deep learning models make their predictions, which in fact promotes greater communication between automated classifiers and human experts [19]. It aims to build AI models that are easier to understand so that they can be trusted and used effectively by humans. Numerous techniques and approaches have been developed by researchers in recent years to enhance the precision and interpretability of deep learning models, and some of these have shown very encouraging results [11]. Class Activation Maps (CAMs), Grad-CAM, Grad-CAM++, Layer-wise Relevance Propagation (LRP), SmoothGrad, RISE method, Concept Activation Vectors (CAVs), DeepTaylor, PatternAttribution, Local Interpret-able-Model Agnostic (LIME), DLIME, SHAP, Anchors, Contrasts, etc. We select Grad-CAM for our research.

3.4.6 Grad-CAM

The Grad-CAM method is a well-known method that may be used to generate a class-specific heatmap by utilizing a specified input image, a CNN that has been trained, and a selected class of interest. It has several similarities with CAM. Grad-CAM may be computed on any CNN architecture provided that the layers can be differentiated from one another. Grad-CAM has been used to problems involving localization with little supervision as well as segmentation with limited supervision [10].

In CAM, the CNN must be updated, which requires retraining. Layers that are fully interconnected must be removed. Instead, before softmax, Global Average Pooling (GAP) is applied. For a specific class c , the final classification score Y^c may be represented as a linear combination of its global average pooling last convolutional layer feature mappings A_k [10] :

$$Y^c = \sum_k w_k^c \sum_i \sum_j A_{ij}^k \quad (3.1)$$

L^c is then calculated for each specific location (i, j) in the class-specific source image as [10] :

$$L_{ij}^c = \sum_k w_k^c * A_{ij}^k \quad (3.2)$$

L_{ij}^c connects directly with the significance of a certain spatial location (i, j) for a specific class c and hence serves as a visual description of the class indicated by the network.

Grad-CAM was designed to handle CAM problems, thus it does not require any retraining or architectural changes. Grad-CAM backpropagations are used to determine weight. The weights w_k^c for a specific feature map A_k and class c are described as follows:

$$w_k^c = \frac{1}{Z} \sum_i \sum_j \frac{\delta Y^c}{\delta A_{ij}^k} \quad (3.3)$$

Here, Z is a constant (pixel count in the activation map). Grad-CAM is thus useful to any deep CNN in which the final Y^c is calculated as follows of the activation maps A_k .

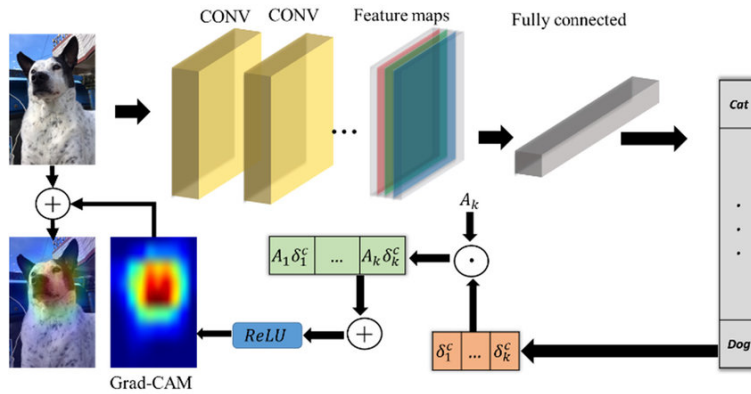


Figure 3.11: *Grad-CAM Architecture [10]*

Chapter 4

Implementation

4.1 System Configuration

For this project, we used Jupyter Notebook. The PC instance has a 3.20 GHz i5 10400 CPU, 32 GB of RAM, and a 12 GB graphics processing unit (GPU) with the model designation "RTX-2060". Just so you know, here is a high-level overview of the system we built our project around. Four different architectures, including Inception V3, ResNet-50 V2, DenseNet-169 and VGG-19 have been utilized in our work.

4.2 Experimental Setup

In TensorFlow, our model library was imported by utilizing the Keras library importer. We have created a base model in which the input shape is the same as our target size (224x224), and we have further included three input channels at the end of the model. In addition, before beginning the training process, we used imagenet as a weighted dataset. We have frozen the layers because there is no need for us to train them at this time. Each of our models was given its own unique iteration that we built. We utilize a data dropout of 0.5 and a 2D global average pooling to get our results. Now that the data are on a plane, it is possible to establish a layer that is completely linked. After that, we created a sequential model in which we used our base models and afterward added three dense batch normalization layers with a total of 64 batches, kernel initialization with uniform parameters, and the remaining two layers each consisting of 32 batches. Dropout was set to 0.5 across all of the layers, and the ReLu activation function was employed throughout the entire process. Due to the fact that our dataset had data on four distinct types of dementia, we chose to use a 6th layer with a total sample size of four and a soft-max function. This is our output layer, and we want to make our predictions using a multinomial probabilistic approach. The number of items in each batch stayed at 8. In order to accomplish this, we made use of Adam, an optimizer whose learning rate changed from an initial 0.002 to a final 0.001 based on the amount of loss that was incurred.

4.3 Performance Matrices

There are 6,400 images total in the dataset, and they are all brain MRIs. To assess our work, which relies on multiclass classification, based just on accuracy would be unfair. Rather, we should consider a wide range of other factors. Classification performance is crucial, so that's how we're measuring how well this model does its job.

4.3.1 Confusion Matrix

The Confusion Matrix is a measure of the classification skills of machine learning systems that assesses the effectiveness of any program. For example, if you have an uneven number of observations in each class or if your dataset has more than two classes, simply looking at classification accuracy may be perplexing. A confusion matrix can therefore provide you with a more precise view of what your classification model gets right and what kinds of errors it makes. The confusion matrix has the following elements:

True Positive: values that were both really positive and predicted to be positive were considered true positives.

True Negative: values are those that were both negative and predicted to be negative.

False Positive: really negative values that were mistakenly seen as good. This issue also goes by the name Type I error.

False Negative: positive values that were incorrectly considered to be negative. This is also known as a Type II error.

4.3.2 Classification Report

The degree to which the efficiency of a model can be estimated is known as its accuracy. Depending on how many examples we give the model, its output might be either positive or negative. This is the formula for verifying accuracy:

$$Accuracy = \frac{(TruePositive + TrueNegative)}{(Truepositive + Falsepositive + Truenegative + Falsenegative)} \quad (4.1)$$

Precision- it assures that the percentage of true positive samples is found among all positive cases. The precision formula:

$$Precision = \frac{(TruePositive)}{(Truepositive + Falsepositive)} \quad (4.2)$$

Recall- it reflects the percentage of true positives predicted out of all positives in the dataset. It is sometimes referred to as "sensitivity." The recall formula:

$$Recall = \frac{(TruePositive)}{(Truepositive + Falsenegative)} \quad (4.3)$$

F1 score- The F1 score assures that accuracy and recall are symmetric. This is the arithmetic mean of recall and accuracy. F1 scoring formula:

$$F1score = \frac{(2PrecisionRecall)}{(Precision + Recall)} \quad (4.4)$$

Chapter 5

Result Analysis and Experimental Evaluation

5.1 Result Analysis

5.1.1 Performance Curve(s)

Matplotlib was used to plot the values of the history of accuracy, history of recall, history of loss, history of precision, and history of F1-score in order to help with the visualization of model metrics. We are able to calculate the accuracy of our model, which will allow us to evaluate how well it functions. Accuracy, in its most fundamental sense, refers to the percentage of inputs for which our model generates correct predictions. In this case, the term "loss" refers to the errors that we make in our predictions, and it is used to fine-tune the weights of our neural network. The proportion of correctly classified positive samples in relation to the total number of positive samples is what we mean when we talk about accuracy. It computes the degree of accuracy with which a model can determine whether or not a sample is positive. The F1 score is a metric that can be used to evaluate how well a model performs on a certain dataset. On the y-axis, we maintained the accuracy, loss, precision, recall, and f1 score, as well as the training and validation accuracy for each example, but we did get rid of all the other epochs.

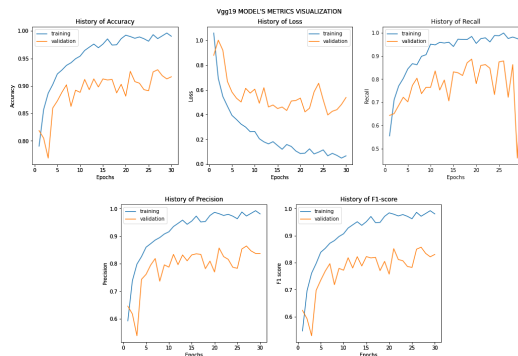


Figure 5.1: *VGG-19 Model's Metric Visualization*

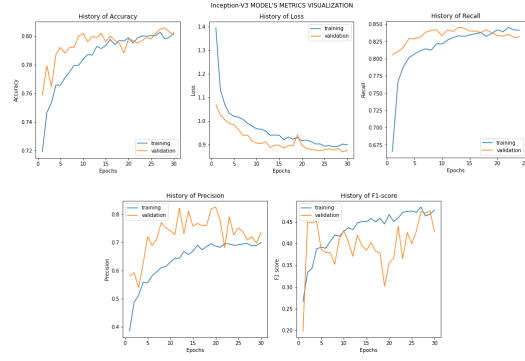


Figure 5.2: *Inception-V3 Model's Metric Visualization*

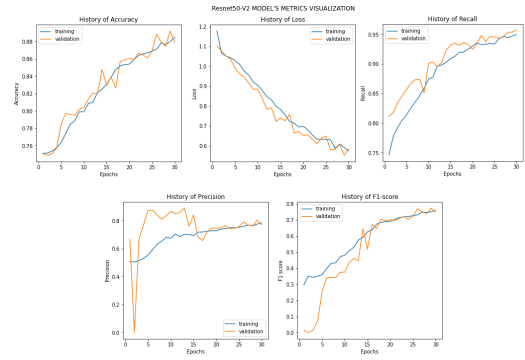


Figure 5.3: *Resnet-50 V2 Model's Metric Visualization*

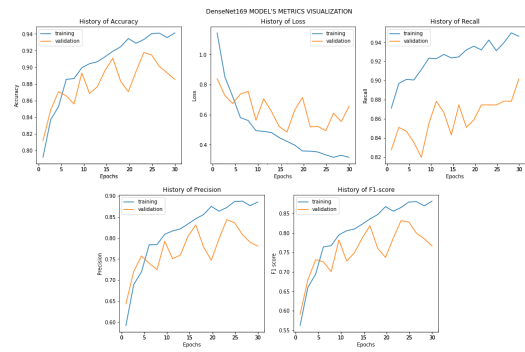


Figure 5.4: *DenseNet-169 Model's Metric Visualization*

5.1.2 Confusion Matrix

The outputs of a classification-based model or system may be described with the help of the confusion matrix. Analyzing the confusion matrix is one method to determine how effective the newly constructed architecture will be. True positives (TP) and True negatives (TN), and False positives (FP) and False Negatives (FN), respectively, are used to indicate the proper and wrong values for each category. This sums up how efficient the model is in detecting the objective and how biased the training process was.

Our confusion matrix has four categories which are mild demented, moderately demented, non-demented, and very mild demented. The anticipated label is on the x-axis, while the true label is on the y-axis.

The confusion matrix of VGG-19, ResNet-50 V2, DenseNet-169, and Inception-v3 is shown in Figures- 5.5, 5.6, 5.7, and 5.8.

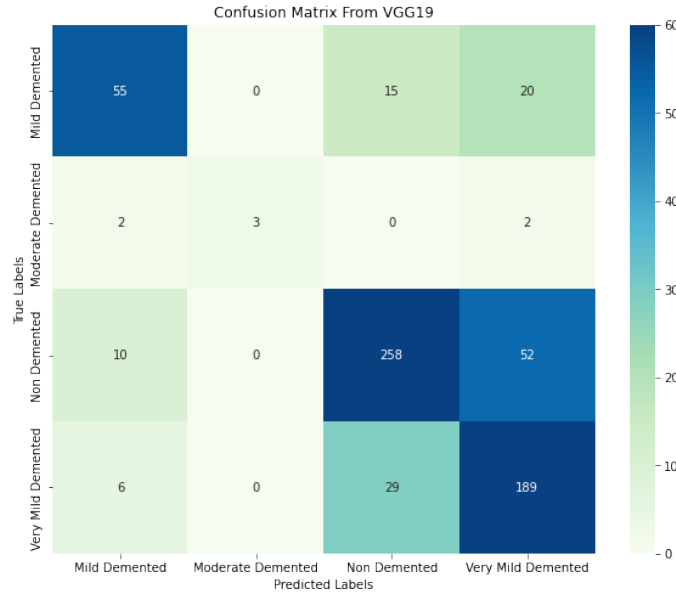


Figure 5.5: *VGG-19 Confusion Matrix*

From figure: 5.5 if we give 90 cases from the Mild Demented class as input, it correctly predicts 55 of those examples from the Mild Demented class and gives 35 examples of incorrect predictions. When we insert images of the moderately demented class, it predicts the highest possible amount of errors in its predictions. In the case of the non-demented class, it is accurately predicting 258 images while giving 62 predictions that are incorrect. Lastly, when putting data of the very mild demented class, it is almost correctly predicting 189 images, while wrongly predicting 35 images.

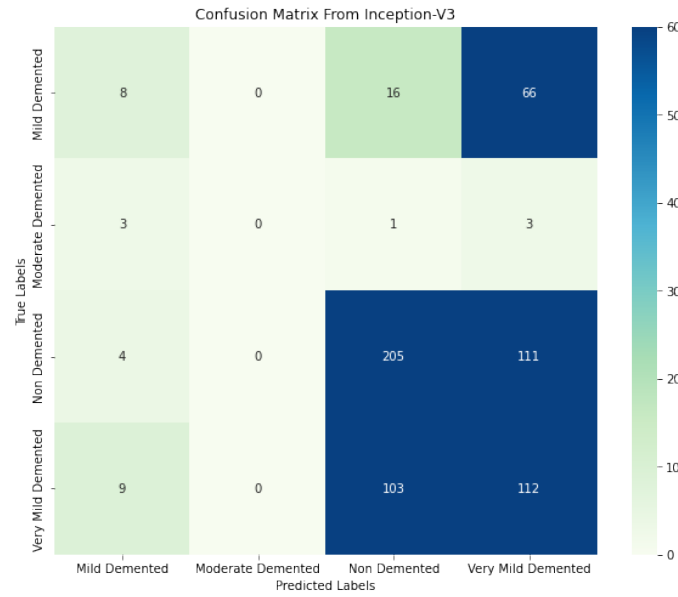


Figure 5.6: *Inception-V3 Confusion Matrix*

By analyzing figure: 5.6 in this case, if we input 90 examples from the Mild Demented class, it correctly predicts 8 cases from that class. 82 images are incorrectly predicted. The most incorrect predictions are made when placing images into the moderate demented class. There are 205 correct predictions for the non-demented class and 115 incorrect ones. Last but not least, when inputting data from a very mild demented class, it almost always gets the predictions of 103 correct predictions and 121 wrong predictions.

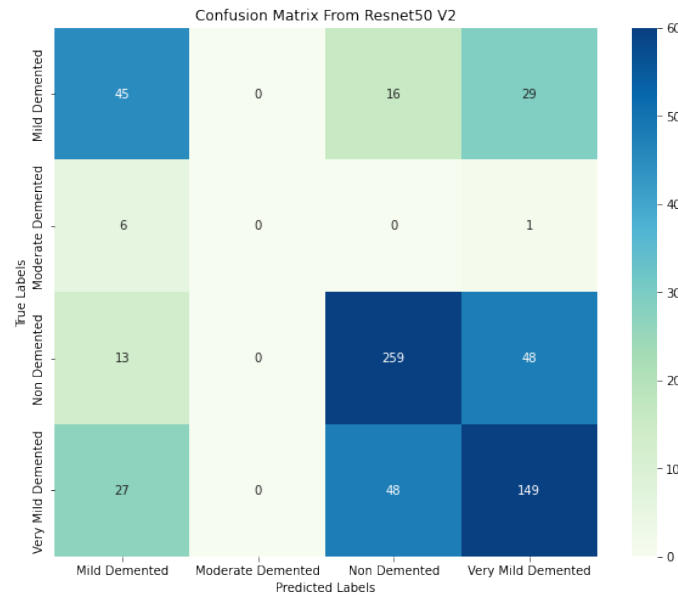


Figure 5.7: *ResNet50 V2 Confusion Matrix*

Similarly, by analyzing figure 5.7 if we provide images of the Mild Demented class as input it can predict 45 images accurately of the Mild Demented class and predict 45 images as a wrong prediction. when we are inserting images in the moderate demented class, it's predicting all numbers of wrong predictions. In the case of the

non-demented class it is predicting 259 images accurately and 61 images as wrong predictions. Lastly, while giving input from a very mild demented class it is almost predicting 149 images as accurately and 75 images as wrong predictions.

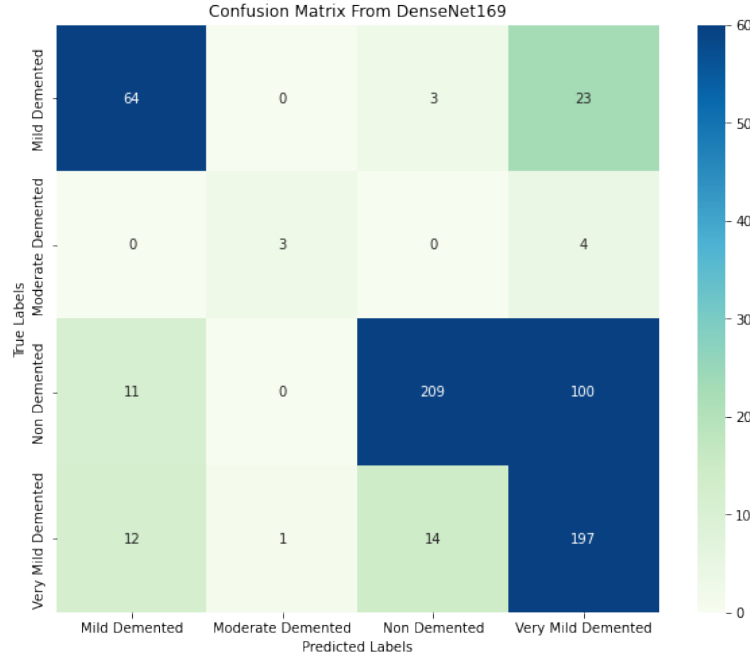


Figure 5.8: *DenseNet-169 Confusion Matrix*

Finally, by analyzing figure 5.8 if we provide the images from the Mild Demented class, it can accurately predict 64 of those images and predict 26 incorrectly. When we insert images into the moderate demented class, it accurately predicts 3 cases while making 4 cases of incorrect predictions. In the instance of the non-demented class, it correctly predicts 209 images while making incorrect predictions for 111 images. Lastly, when a very mild demented class is given as input, it almost predicts 197 images as accurate and 27 images as wrong.

5.1.3 Performance Evaluation

We trained four different models with our dataset and evaluated the categorization and training accuracy before trying to come up with an explanation for the classification or prediction of specific MRI images. Our dataset was divided into four categories: non-demented, very mildly demented, mildly demented, and moderately demented.

The results of the four models in training and validation after 30 epochs is shown in the tables below. We intended to reveal the findings for further comprehension, but the accuracy does not improve much over longer periods.

Table 5.1: TABLE 1

VGG-19 Corresponding Numeric Metric Score

Train/Val	Epochs	Accuracy	Loss	Precision	Recall
Train	30 Epochs	0.9908	0.1324	0.9827	0.9806
Validation	30 Epochs	0.9265	0.3783	0.8600	0.9730

Table 5.2: TABLE 2

Inception-V3 Corresponding Numeric Metric Score

Train/Val	Epochs	Accuracy	Loss	Precision	Recall
Train	30 Epochs	0.8024	0.8988	0.7001	0.3616
Validation	30 Epochs	0.8010	0.8767	0.7364	0.3294

Table 5.3: TABLE 3

ResNet-50 V2 Corresponding Numeric Metric Score

Train/Val	Epochs	Accuracy	Loss	Precision	Recall
Train	30 Epochs	0.8847	0.5738	0.7851	0.7637
Validation	30 Epochs	0.8784	0.5861	0.7695	0.7686

Table 5.4: TABLE 4

DenseNet-169 Corresponding Numeric Metric Score

Train/Val	Epochs	Accuracy	Loss	Precision	Recall
Train	30 Epochs	0.9475	0.1511	0.9068	0.9464
Validation	30 Epochs	0.8918	0.7010	0.7980	0.9020

5.2 Comparison between the Deep Learning Models

To perform our research, we used VGG-19, InceptionV3, ResNet-50 V2, and DenseNet-169. Clearly, we were able to produce at least a decent result. While we believe that accuracy alone is not a sufficient metric for judging the success of our research, it is possible that this is the case. We achieved an accuracy of 87.84% with ResNet-50 V2. The 92.65% accuracy we achieved with VGG-19 is quite good. We obtained 80.10% accuracy using the Inception-V3 model, while an even higher 89.18% accuracy was achieved with the DenseNet-169 model. Among the four models, VGG-19 clearly provides the most accurate result. Apart from that, the accuracy of the results produced by DenseNet-169 is quite close to that of VGG-19. The performance of Inception V3 is significantly lower than that of competing models. If we had found more relevant data for our investigation, we might have achieved better

results. Thus, after careful consideration, we can decide on VGG-19 as the optimal model for our research.

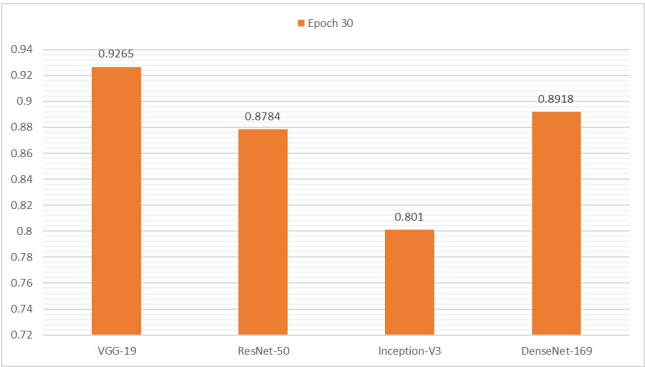


Figure 5.9: *Accuracy evaluations of four different models*

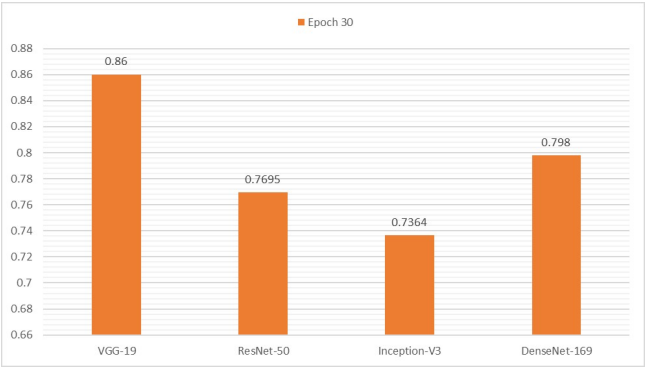


Figure 5.10: *Precision evaluations of four different models*

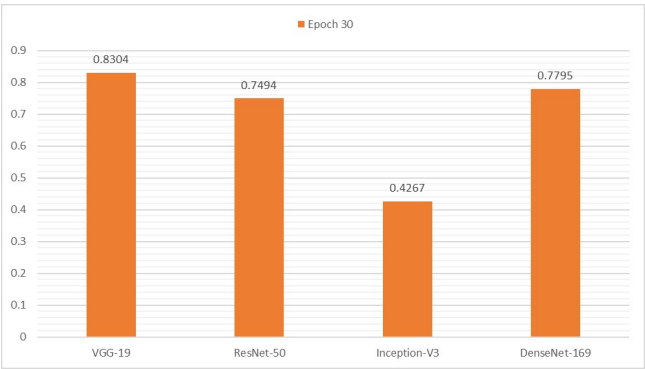


Figure 5.11: *F1 Score evaluations of four different models*

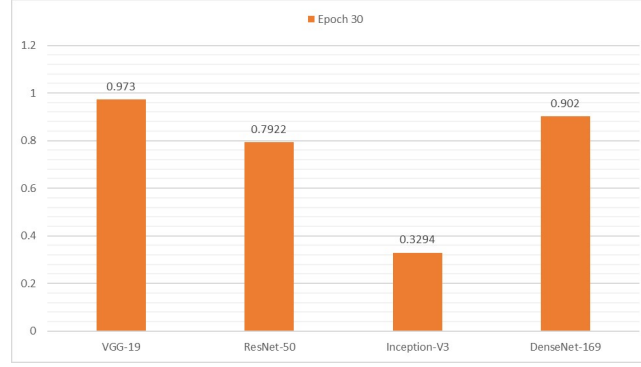


Figure 5.12: *Recall evaluations of four different models*

5.2.1 Result Metrics

We can observe from Figure 5.13 that the precision for the mild demented class is 0.72, the recall is 0.67, and the f1 score is 0.69 if we look at the result matrix for the VGG-19 model on our dataset. Precision is 1, recall is 0.29, and f1 score is 0.44 for the moderate demented class. Again, the f1 score is 0.78, recall is 0.68, and precision is 0.91 for the non-demented class. The precision, recall, and f1 score for the very mild demented class are 0.62, 0.88, and 0.73, respectively. The expected levels of precision for accuracy, macro average, and weighted avg true level are 0.74, 0.81, and 0.78, respectively. In addition, the recall at the actual level is 0.74, the macro average is 0.63, the weighted average is 0.74, and the f1 score is 0.74, 0.66, and 0.74.

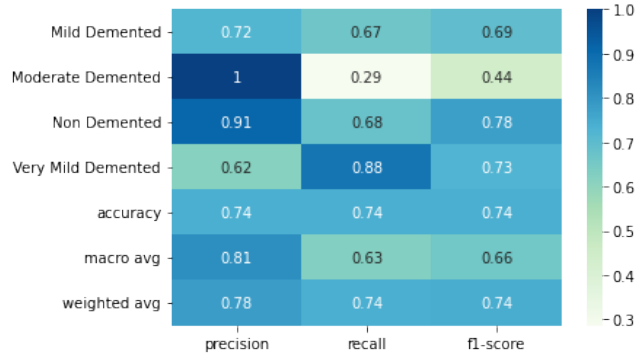


Figure 5.13: *Result Metrics for best fit model(VGG-19)*

5.3 Result Analysis with Grad-CAM

Finally, we applied GradCam to our best-fit VGG-19 model. The regions that determine the predictions made by VGG19 can be visualized by looking at the images that are provided below :

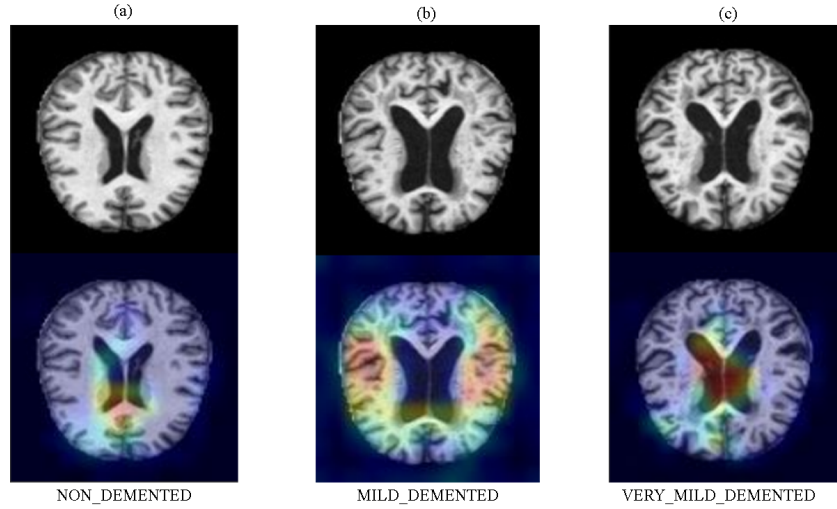


Figure 5.14: *Grad-CAM interpretation of the prediction made by VGG19 when an image of (a) Non-Demented, (b) Mild-Demented, and (c) Very Mild-Demented is provided as input*

In Figure 5.14, the images Figure 5.14 (a) are from the non-demented class. The image Figure 5.14 (b) is of people with mild dementia, and the picture Figure 5.14 (c) is of people with very mild dementia. By evaluating this interpretation that was made by Grad-CAM, we are able to interpret the prediction made by VGG19 because we can now see that it is looking at the correct regions (regions having a red effect) while predicting image in 5.14 (b) belongs to the Mild-demented class. This is because we can now see that it is looking at the regions that have the red effect. In a similar manner, we can observe from Figure 5.14 (c) that VGG19 is looking at the appropriate region while making its prediction regarding the image that belongs to the very mild demented class.

On the other hand, if we look at the image in Figure 5.14 (a), we can see that even though VGG19 is correctly classifying this image of non-demented as non-demented, the region it is looking at to make this prediction is not correct overall. This can be seen by the fact that even though it is correctly classifying the image as non-demented, it is still incorrect. It is looking at regions that contain other regions that have not been affected.

Chapter 6

Conclusion

6.1 Conclusion

Alzheimer’s disease is a neurological disease that progressively gets worse over time and cannot be cured. It eventually causes damage to brain cells. Around 55 million people are suffering from Alzheimer’s disease on a worldwide scale. It is estimated that this number would nearly double every 20 years, reaching 78 million in the year 2030 and 139 million in the year 2050 [37]. Because so little is known about how to avoid the condition, it is important that we work toward predicting or identifying it as early as possible, and that we also make an effort to make treatment more accessible and understandable to an ever-increasing number of people. As a result of this, we use a number of different neural network models to analyze and provide predictions of the early stages of Alzheimer’s disease. We showed a number of papers that were connected to this topic as well as recent experiments that were conducted on a variety of datasets. During the course of our research, we used ResNet-50 V2, VGG19, DenseNet-169, and Inception V3 to process the data, and we presented the results with the Grad-CAM-based XAI framework. 70 percent of our data was put toward training, 20 percent toward testing, and 10 percent toward validation. To conclude, our predictions for the four classes had an accuracy of 92.65% when we used VGG-16, 89.18% when we used DenseNet-169, 87.84% when we used ResNet-50 V2, and 80.10% when we used Inception-v3. Furthermore, this demonstrates promising results that may be improved upon and utilized in multiple circumstances. The adaptability of our Grad-CAM basic architecture is not only a method for making low-level data simpler to use and comprehend, but it is also a principle that can be used for a number of other elements of the data processing sector.

6.2 Limitations

During the process of working on this research, we came across a number of difficulties and limitations. To begin, we made an effort to get MRI data from a local institution in Bangladesh so that we could include the statistics and situations that are particular to the region. However, due to time constraints, we were unable to gather the essential data. Despite the size of the accuracy percentages our training models have yielded, there is still room for growth as our prime objective was to get values greater than 94%. Last but not least, the loss margin is another area in

which the values were lower than what is considered to be acceptable. We might be able to reduce the loss in this area by analyzing some of the information that we get from the models and trying to adjust it further for greater accuracy using the various regularization approaches that are available, such as L1 and L2. Because the approach we are focused on is directed primarily at the health industry, higher accuracy and lower data loss are important for presenting patients with a precise Alzheimer's diagnosis.

6.3 Future Work

When it comes to our research and the work that we did, the models that we developed, improved and presented achieved a high level of accuracy. Our most recent findings have the ability to act as a basis for further research and study on Alzheimer's disease in Bangladesh. Our primary objective is to first improve the models by modifying and enhancing them in order to reach higher levels of consistency and accuracy. Another area that has space for improvement is the proportion of data that is lost while it is being processed, which is something that we will work to minimize in order to make the process more effective. In addition, Grad-CAM is not able to correctly identify objects in an image if the image contains many instances of the same class. This is a limitation of the Grad-CAM system. Grad-CAM determines the weight by dividing Z , which represents the size of the feature map. The weight decreases as the response or area of the reaction decreases. The mentioned problems can be resolved with Grad-CAM++ because of its more advanced backpropagation. So, in the future, we will utilize Grad-CAM++ instead of Grad-CAM to overcome this issue.

Bibliography

- [1] S. Wold, K. H. Esbensen, and P. Geladi, “Principal component analysis,” *Comprehensive Chemometrics*, 1987.
- [2] A. D. Baddeley, S. Bressi, S. D. Sala, R. H. Logie, and H. R. Spinnler, “The decline of working memory in alzheimer’s disease. a longitudinal study,” *Brain: a journal of neurology*, vol. 114 (Pt 6), pp. 2521–42, 1991.
- [3] M. B. Graeber, S. Kösel, R. Egensperger, *et al.*, “Rediscovery of the case described by alois alzheimer in 1911: Historical, histological and molecular genetic analysis,” *Neurogenetics*, vol. 1, pp. 73–80, 1997.
- [4] C. R. Jack, M. A. Bernstein, N. C. Fox, *et al.*, “The alzheimer’s disease neuroimaging initiative (adni): Mri methods,” *Journal of Magnetic Resonance Imaging*, vol. 27, 2008.
- [5] J. Nagi, F. Ducatelle, G. A. D. Caro, *et al.*, “Max-pooling convolutional neural networks for vision-based hand gesture recognition,” *2011 IEEE International Conference on Signal and Image Processing Applications (ICSIPA)*, pp. 342–347, 2011.
- [6] S. Liu, S. Liu, W. (Cai, S. Pujol, R. Kikinis, and D. D. Feng, “Early diagnosis of alzheimer’s disease with deep learning,” *2014 IEEE 11th International Symposium on Biomedical Imaging (ISBI)*, pp. 1015–1018, 2014.
- [7] G. Huang, Z. Liu, and K. Q. Weinberger, “Densely connected convolutional networks,” *2017 IEEE Conference on Computer Vision and Pattern Recognition (CVPR)*, pp. 2261–2269, 2016.
- [8] S. Sarraf and G. Tofighi, “Classification of alzheimer’s disease using fmri data and deep learning convolutional neural networks,” *ArXiv*, vol. abs/1603.08631, 2016.
- [9] V. Feng, “An overview of resnet and its variants,” 2017.
- [10] A. Chattopadhyay, A. Sarkar, P. Howlader, and V. N. Balasubramanian, “Grad-cam++: Improved visual explanations for deep convolutional networks.,” 2018.
- [11] F. K. Dosilovic, M. Bri, and N. Hlupic, “Explainable artificial intelligence: A survey,” *2018 41st International Convention on Information and Communication Technology, Electronics and Microelectronics (MIPRO)*, pp. 0210–0215, 2018.
- [12] H. Padole, S. D. Joshi, and T. K. Gandhi, “Early detection of alzheimer’s disease using graph signal processing on neuroimaging data,” *2018 2nd European Conference on Electrical Engineering and Computer Science (EECS)*, pp. 302–306, 2018.

- [13] Y. Shi and D. M. Holtzman, “Interplay between innate immunity and alzheimer disease: Apoe and trem2 in the spotlight,” *Nature Reviews Immunology*, vol. 18, pp. 759–772, 2018.
- [14] Y. Zheng, C. Yang, and A. Merkulov, “Breast cancer screening using convolutional neural network and follow-up digital mammography,” May 2018, p. 4.
- [15] Y. A. Hamad, K. Simonov, and M. B. Naeem, “Detection of brain tumor in mri images, using a combination of fuzzy c-means and thresholding,” *Int. J. Adv. Pervasive Ubiquitous Comput.*, vol. 11, pp. 45–60, 2019.
- [16] R. Jain, N. Jain, A. Aggarwal, and D. J. Hemanth, “Convolutional neural network based alzheimer’s disease classification from magnetic resonance brain images,” *Cognitive Systems Research*, vol. 57, pp. 147–159, 2019.
- [17] T. Jo, K. Nho, and A. J. Saykin, “Deep learning in alzheimer’s disease: Diagnostic classification and prognostic prediction using neuroimaging data,” *Frontiers in Aging Neuroscience*, vol. 11, 2019.
- [18] H. Li and Y. Fan, “Early prediction of alzheimer’s disease dementia based on baseline hippocampal mri and 1-year follow-up cognitive measures using deep recurrent neural networks,” *2019 IEEE 16th International Symposium on Biomedical Imaging (ISBI 2019)*, pp. 368–371, 2019.
- [19] E. Tjoa and C. Guan, “A survey on explainable artificial intelligence (xai): Toward medical xai,” *IEEE Transactions on Neural Networks and Learning Systems*, vol. 32, pp. 4793–4813, 2019.
- [20] M. Yamazaki, A. Kasagi, A. Tabuchi, *et al.*, “Yet another accelerated sgd: Resnet-50 training on imagenet in 74.7 seconds,” *ArXiv*, vol. abs/1903.12650, 2019.
- [21] “2020 alzheimer’s disease facts and figures,” *Alzheimer’s & Dementia*, vol. 16, 2020.
- [22] X. Bi, S. Li, B. Xiao, Y. Li, G. Wang, and X. Ma, “Computer-aided alzheimer’s disease diagnosis by an unsupervised deep learning technology,” *Neurocomputing*, vol. 392, pp. 296–304, 2020.
- [23] G. Folego, M. Weiler, R. Casseb, R. Pires, and A. Rocha, “Alzheimer’s disease detection through whole-brain 3d-cnn mri,” *Frontiers in Bioengineering and Biotechnology*, vol. 8, 2020.
- [24] E. Hussain, M. Hasan, S. Z. Hassan, T. H. Azmi, M. A. Rahman, and M. Z. Parvez, “Deep learning based binary classification for alzheimer’s disease detection using brain mri images,” *2020 15th IEEE Conference on Industrial Electronics and Applications (ICIEA)*, pp. 1115–1120, 2020.
- [25] W. H. Organization, “Alzheimer’s and dementia in bangladesh,” 2020.
- [26] M. Raju, T. V. Sudila, V. P. Gopi, and V. S. Anitha, “Classification of mild cognitive impairment and alzheimer’s disease from magnetic resonance images using deep learning,” *2020 International Conference on Recent Trends on Electronics, Information, Communication & Technology (RTEICT)*, pp. 52–57, 2020.

- [27] N. Roy, A. Hassan, R. Alom, M. H. R. Rajib, and K. A. Al-Mamun, “The situation of alzheimer’s disease in bangladesh: Facilities, expertise, and awareness among general people,” 2020.
- [28] A. Yiğit and Z. Işık, “Applying deep learning models to structural mri for stage prediction of alzheimer’s disease,” *Turkish J. Electr. Eng. Comput. Sci.*, vol. 28, pp. 196–210, 2020.
- [29] Anonymous, “2021 alzheimer’s disease facts and figures,” *Alzheimer’s & Dementia*, vol. 17, 2021.
- [30] M. Bansal, M. Kumar, M. Sachdeva, and A. Mittal, “Transfer learning for image classification using vgg19: Caltech-101 image data set,” *Journal of Ambient Intelligence and Humanized Computing*, pp. 1–12, 2021.
- [31] P. G. Brindha, M. Kavinraj, P. Manivasakam, and P. U. Prasanth, “Brain tumor detection from mri images using deep learning techniques,” *IOP Conference Series: Materials Science and Engineering*, vol. 1055, 2021.
- [32] A. W. Bhade and G. Bamnote, “Comparison of pre-processing and feature extraction techniques for alzheimer detection using mri images,” *2022 Fifth International Conference on Computational Intelligence and Communication Technologies (CCICT)*, pp. 42–48, 2022.
- [33] S. Fouladi, A. A. Safaei, N. I. Arshad, M. J. Ebadi, and A. Ahmadian, “The use of artificial neural networks to diagnose alzheimer’s disease from brain images,” *Multimedia Tools and Applications*, vol. 81, pp. 37 681–37 721, 2022.
- [34] Rukhsar and S. K. Upadhyay, “Deep transfer learning-based rice leaves disease diagnosis and classification model using inceptionv3,” *2022 International Conference on Computational Intelligence and Sustainable Engineering Solutions (CISES)*, pp. 493–499, 2022.
- [35] D. S. Shastri, “Alzheimer’s dataset (4 class of images),” kaggle, 2022.
- [36] A. Ukil, L. Marin, and A. Jara, “Adv-resnet: Residual network with controlled adversarial regularization for effective classification of practical time series under training data scarcity problem,” *2022 International Joint Conference on Neural Networks (IJCNN)*, pp. 1–8, 2022.
- [37] “Alzheimer’s disease international- dementia statistics,” 2023.